AIP | Applied Physics Letters

High- Q transverse-electric/transverse-magnetic photonic crystal nanobeam cavities

Murray W. McCutcheon, Parag B. Deotare, Yinan Zhang, and Marko Lončar

Citation: Applied Physics Letters **98**, 111117 (2011); doi: 10.1063/1.3568897
View online: http://dx.doi.org/10.1063/1.3568897
View Table of Contents: http://scitation.aip.org/content/aip/journal/apl/98/11?ver=pdfcov
Published by the AIP Publishing

High-*Q* transverse-electric/transverse-magnetic photonic crystal nanobeam cavities

Murray W. McCutcheon,[a] Parag B. Deotare, Yinan Zhang, and Marko Lončar
School of Engineering and Applied Sciences, Harvard University, Cambridge, Massachusetts 02138, USA

(Received 17 December 2010; accepted 24 February 2011; published online 18 March 2011)

We experimentally demonstrate high quality factor dual-polarized photonic crystal nanobeam cavities. The free-standing nanobeams are fabricated in a 500 nm thick silicon layer, and are probed using both tapered optical fiber and free-space resonant scattering set-ups. We measure Q factors greater than 10^4 for both transverse magnetic (TM) and transverse electric modes, and observe fiber transmission drops as large as $1-T=0.8$ at the TM mode resonances. © *2011 American Institute of Physics*. [doi:10.1063/1.3568897]

There has been significant interest in nanobeam photonic crystal cavities in the last three years. Although proposed more than a decade ago,[1] it was only recently shown that this architecture was capable of supporting ultrahigh Q-factor cavities with dimensions on the order of a cubic wavelength in material.[2–4] Since then, there have been a host of demonstrations, including optomechanical crystals,[5] operation in the visible,[6–8] low-power reconfigurable switches,[9] biosensors,[10,11] and nanocavities strongly coupled to waveguides[12,13] and lasers.[14–16]

Recently, we showed theoretically that nanobeams could be engineered to have both transverse electric (TE) and transverse magnetic (TM) stopbands, provided the nanobeam is thick enough to support TM guided modes.[17] High Q-factor cavity modes can be designed for both polarizations *simultaneously* by using an appropriate lattice tapering. By tuning the aspect ratio of the nanobeam (namely the height and width), the energy separation of the modes can be tuned. Dual-polarized nanocavities have many potential applications in chip-scale nonlinear optics. In particular, we have recently proposed such a system for single-photon frequency conversion in III–V materials.[18,19] These devices also raise the intriguing prospect of photonic crystal quantum cascade lasers,[20,21] for which the radiation is TM-polarized.

In this letter, we report the experimental observation of TE/TM dual-mode cavities in silicon. Our cavity design exploits the principles we (and others) have outlined in prior work.[3,4,17,22–24] We have shown that nanobeam cavities can be designed to have both TE and TM modes with Quality factors exceeding 10^6 but this requires a very thick structure with thickness:width:period ratio of 3:1:1.[17] Here, given our silicon device layer thickness of 500 nm and our operating wavelength near 1500 nm, the cavities were designed with TE and TM modes with bare (intrinsic) Q factors of 7×10^6 and 1.2×10^5, and mode volumes of 0.56 and 1.37, respectively. The nanocavities have a designed width of 380–400 nm, hole pitch $a=330$ nm, radius $r/a=0.265$, and a symmetric six-period taper to a pitch of $0.84a$ in the center of the cavity. The TE and TM modes are separated by 50 nm with the TE mode at higher energy. The field intensity profiles for the modes extracted from three-dimensional (3D) finite-difference time-domain (FDTD) simulations are shown in Fig. 1.

Because TM modes have the dominant electric field component oriented orthogonal to the device plane, they must be excited via evanescent[25] or end-fire waveguide coupling techniques.[26] They cannot be readily probed from free-space,[27] since, like an electric dipole, they do not radiate parallel to the axis of the dipole moment. By contrast, in our geometry, the TE-cavity is only weakly coupled to a tapered optical fiber. This is due to the rather thick nanobeam, which causes the overlap with the fiber mode to be significantly reduced from what is typically the case for thin nanobeams.[5] To understand this polarization-dependent coupling, consider the electric field strength of both TE and TM modes as a function of z from the middle of the cavity, as plotted in Fig. 2. In the evanescent region (to the right of the dashed line), the TM E-field is about twice the magnitude of the TE E-field, which is a consequence of the field boundary conditions. Since the electric field of the TM mode is dominantly perpendicular to the silicon/fiber interface, it must satisfy the boundary condition $\epsilon_1 E_{z,1}=\epsilon_2 E_{z,2}$, where 1 denotes the silicon and 2 the fiber. On the other hand, the TE mode fields are oriented parallel to the interface, and must therefore be continuous across the boundary, i.e., $E_{y,1}=E_{y,2}$. By this simple argument, we expect an enhanced fiber coupling to the TM modes.

In light of these observations, we use two complimentary techniques in order to probe our TE-TM cavities. First, we employ a tapered fiber optical set-up. We pull an SMF-28 telecom fiber heated with a hydrogen torch to a diameter close to 1 μm. The fiber is mounted in a U-shaped configuration, which self-tensions the taper region and allows the

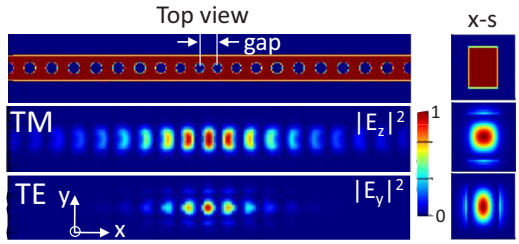

FIG. 1. (Color online) Field intensity profiles $|E_z|^2$ ($|E_y|^2$) for the TM (TE) modes shown from the top and in cross-section (x-s). The TM mode has a larger mode volume, and its field extends significantly above the cavity.

[a]Electronic mail: murray@seas.harvard.edu.

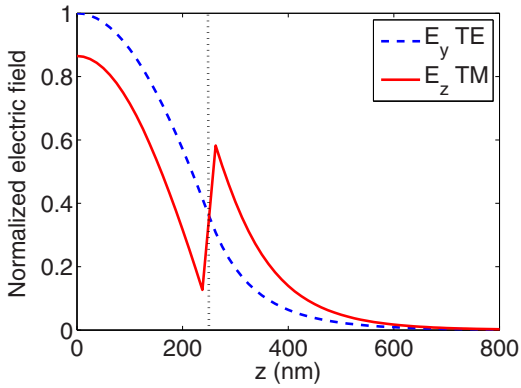

FIG. 2. (Color online) Comparison between the dominant electric field components of the two modes (normalized to the same energy) as a function of distance perpendicular to the device plane (z=0 denotes the middle of the cavity, and the dashed line marks the top surface).

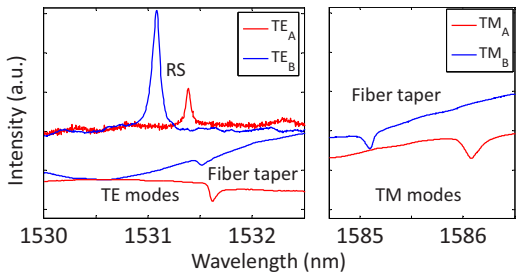

FIG. 4. (Color online) Spectra from two cavities, A and B, each of which supports high Q-factor modes at both TE and TM polarizations ($Q_{TE,A}$ =28 000, $Q_{TE,B}$=18 000, $Q_{TM,A}$=10 000, and $Q_{TM,B}$=19 000). The fiber taper spectra reveal both features, whereas the RS spectra resolve only the TE modes, since they couple to radiation normal to the device plane. The color of each spectrum indicates the cavity being probed (red—A, blue—B). In the left panel, the fiber spectra are redshifted due to the presence of the fiber.

fiber to be brought into close proximity with the sample surface. We then dimple the fiber by using a bare fiber as a mold, and applying pressure to the narrowest part of the taper while heating the contact region.[28] The dimple, which is typically about 10 μm in depth, as shown in Fig. 3, creates a local evanescent probe to the nanocavity of interest. The tapered fiber is spliced into an optical set-up, and its location with respect to the sample is precisely positioned using motorized stages with 50 nm encoder resolution (Surugu Seiki). The photodiode signal (Thorlabs Det010FC with a 1 kΩ load resistor) is passed through a low noise Stanford pre-amplifier and low-pass filtered at 1 kHz before computer acquisition.

The second spectroscopy technique we use is a cross-polarized resonant scattering (RS) set-up, in which light incident from normal to the plane of the sample is strongly focused by a 100× objective and the reflected signal detected in the cross polarization.[27] This method allows us to confirm the polarization of the modes detected by the tapered fiber, since it is only sensitive to the TE modes.

The cavities were fabricated with standard e-beam lithography and reactive ion etching methods, as described previously.[24]

Figure 4 shows spectra from two different high-Q, TE-TM nanocavities. The cavities are nominally identical except that the filling fraction of the air holes of cavity A (red) is slightly smaller than that of cavity B (blue). These cavities are not actually fabricated according to the optimal design, but are intentionally detuned in order to lower the

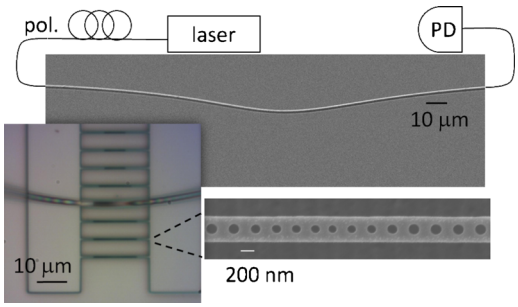

FIG. 3. (Color online) SEM image of a dimpled fiber taper and a schematic of the optical set-up (PD—photodiode). The optical image (left) shows the dimpled fiber taper in direct contact with a nanobeam cavity, which is shown in greater detail in the SEM inset.

Q-factor of the TE mode and increase its visibility in the spectra. This is achieved by reducing the gap between the two central holes by 20 nm (see Fig. 1). However, the Q factors still exceed 10^4 for each of the modes in the figure. We used a similar detuning method in previous work[24] to predictably shift the Q-factor and operating wavelength of our nanobeam cavities. Using scanning electron microscope (SEM) images of the fabricated structure, we perform 3D-FDTD simulations of cavity A, and predict unloaded Q factors of $Q_{TE,A}$=27 000 and $Q_{TM,A}$=60 000.

Measurements from both the fiber taper and RS set-ups are shown in the same graph. The TE mode of cavity A at 1531.4 nm has a bare Q-factor of 28 000, as determined by RS, in good agreement with the simulated value (cf. cavity B, $Q^{exp}_{TE,B}$=18 000). The TM modes near 1585 nm have loaded Q-factors of ~10 000, less than the predicted intrinsic Q value, which reflects in part the extent to which the fiber loads the cavity. As expected, the TE modes of the cavities can be probed using both experimental methods, whereas the TM modes couple only to the fiber taper. The fiber transmission spectra are acquired by touching the fiber to the cavity (as visible in the optical image in Fig. 3), which was found to provide greater stability and repeatability compared to evanescent coupling from the air. In the fiber data, the modes are revealed as dips since light which is "dropped" from the fiber into the cavity can couple into other loss-channels of the cavity (e.g., scattering into free space). In the RS spectra, the modes appear as peaks on the nonresonant background (although both dips and Fano features[29] are possible). The Lorentzian lineshapes in the RS spectra are centered at the bare (unloaded) cavity resonance, and their widths give the unloaded Q-factors of the cavities. The fiber spectra are slightly redshifted due to the perturbative effects of the silica fiber, and the amount of the shift depends on how exactly the fiber contacts the particular cavity.

Although the strength of the fiber coupling to both the TE and TM modes is similar in Fig. 4, in general we observe a greatly enhanced coupling to the TM modes compared to the TE modes in our fabricated structures. Figure 5(a) shows a single spectrum (cropped to highlight the modes of interest) in which the coupling to the TE mode is only about $1-T$=0.05, whereas for the TM mode it is $1-T$=0.3. We have not observed transmission drops greater than $1-T$=0.1 (T =0.9) for the TE modes, whereas drops of 0.3–0.4 are quite typical for TM modes. This polarization-dependent coupling

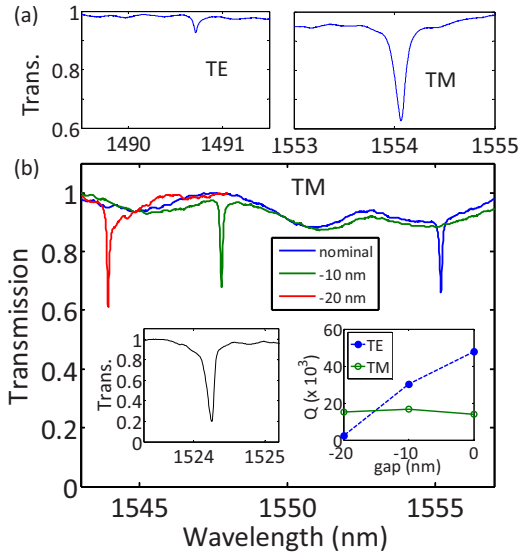

FIG. 5. (Color online) (a) TE-TM spectrum highlighting the polarization-dependent coupling. (b) TM spectra from three cavities which are well coupled to the fiber taper ($1-T=0.3-0.4$). The spacing (gap) between the central two holes of the cavity (see legend) varies the resonant wavelength but has little effect on the TM Q-factors (see right inset), in contrast to the TE modes (Q_{TE} extracted from RS data). The left inset shows the very large coupling ($1-T=0.8$) of another similar TM cavity mode. The spectra are all acquired with the fiber in contact with the cavity.

is not surprising in light of the field profiles shown in Fig. 2. Figure 5(b) shows TM spectra from a sequence of three cavities similar to the one in Fig. 5(a), all of which exhibit large coupling of $1-T=0.3-0.4(T=0.6-0.7)$. Each of these cavities has a width of 360 nm, $r/a=0.27$, and a six-hole cavity taper, as described earlier. The three cavities differ only in the gap between the central two holes of the cavity. The resonance blueshifts as the gap is decreased, as expected. The Q-factor ($\sim$15 000) varies little for the TM modes over this range, whereas the TE modes are highly sensitive to the gap (see inset) due to their tight confinement in the cavity center. These trends agree well with FDTD modeling and our previous work;[3,24] overall, the measured Q values are lower than in simulation due to fabrication imperfections. The dip can be as large as $1-T=0.8(T=0.2)$, as shown in the left inset of Fig. 5 while maintaining a Q-factor greater than 10^4, which is very promising for fiber-coupled applications. A more detailed analysis of the polarization-dependent coupling using coupled mode theory[30,31] supports the simple argument based on Fig. 2, and shows that the TM mode in thick membrane cavities is much better phase-matched to the fundamental fiber mode than the TE mode.

In conclusion, using a combination of fiber taper and RS spectroscopy, we have experimentally demonstrated high Q-factor, dual-polarized TE-TM photonic crystal nanobeam cavities in silicon. The modes are separated by 50 nm, and have Q-factors greater than 10^4. We observe large coupling of the TM modes in fiber taper transmission measurements, which we attribute to the significant evanescent tail of the TM mode above the cavity. We anticipate this phenomenon could be exploited for certain applications, such as biosensing.[32] More generally, we foresee TE-TM nanocavities playing an enabling role in integrated applications, such as nonlinear wavelength conversion and quantum-cascade lasers.

[1]J. S. Foresi, P. R. Villeneuve, J. Ferrara, E. R. Thoen, G. Steinmeyer, S. Fan, J. D. Joannopoulos, L. C. Kimerling, H. I. Smith, and E. P. Ippen, Nature (London) **390**, 143 (1997).
[2]M. Notomi, E. Kuramochi, and H. Taniyama, Opt. Express **16**, 11095 (2008).
[3]M. W. McCutcheon and M. Lončar, Opt. Express **16**, 19136 (2008).
[4]J. Chan, M. Eichenfield, R. Camacho, and O. Painter, Opt. Express **17**, 3802 (2009).
[5]M. Eichenfield, J. Chan, R. Camacho, K. J. Vahala, and O. Painter, Nature (London) **462**, 78 (2009).
[6]Y. Gong and J. Vučković, Appl. Phys. Lett. **96**, 031107 (2010).
[7]M. Khan, T. Babinec, M. W. McCutcheon, P. Deotare, and M. Lončar, Opt. Lett. **36**, 421 (2011).
[8]M. M. Murshidy, A. M. Adawi, P. W. Fry, and D. G. Lidzey, Appl. Phys. Lett. **97**, 153303 (2010).
[9]I. W. Frank, P. B. Deotare, M. W. McCutcheon, and M. Lončar, Opt. Express **18**, 8705 (2010).
[10]A. Di Falco, L. O'Faolain, and T. F. Krauss, Appl. Phys. Lett. **94**, 063503 (2009).
[11]B. Wang, M. A. Dundar, R. Notzel, F. Karouta, S. He, and R. W. van der Heijden, Appl. Phys. Lett. **97**, 151105 (2010).
[12]Q. Quan, P. B. Deotare, and M. Lončar, Appl. Phys. Lett. **96**, 203102 (2010).
[13]A. R. M. Zain, M. Gnan, H. M. H. Chong, M. Sorel, and R. M. De La Rue, IEEE Photon. Technol. Lett. **20**, 6 (2008).
[14]Y. Halioua, A. Bazin, P. Monnier, T. J. Karle, I. Sagnes, G. Roelkens, D. V. Thourhout, F. Raineri, and R. Raj, J. Opt. Soc. Am. B **27**, 2146 (2010).
[15]Y. Zhang, M. Khan, Y. Huang, J. H. Ryou, P. B. Deotare, R. Dupuis, and M. Lončar, Appl. Phys. Lett. **97**, 051104 (2010).
[16]Y. Gong, B. Ellis, G. Shambat, T. Sarmiento, J. S. Harris, and J. Vučković, Opt. Express **18**, 8781 (2010).
[17]Y. Zhang, M. W. McCutcheon, I. B. Burgess, and M. Lončar, Opt. Lett. **34**, 2694 (2009).
[18]M. W. McCutcheon, D. E. Chang, Y. Zhang, M. D. Lukin, and M. Lončar, Opt. Express **17**, 22689 (2009).
[19]I. B. Burgess, Y. Zhang, M. W. McCutcheon, A. W. Rodriguez, J. Bravo-Abad, S. G. Johnson, and M. Lončar, Opt. Express **17**, 20099 (2009).
[20]Y. Wakayama, A. Tandaechanurat, S. Iwamoto, and Y. Arakawa, Opt. Express **16**, 21321 (2008).
[21]M. Lončar, B. G. Lee, L. Diehl, M. A. Belkin, F. Capasso, M. Giovannini, J. Faist, and E. Gini, Opt. Express **15**, 4499 (2007).
[22]P. Lalanne and J. P. Hugonin, IEEE J. Quantum Electron. **39**, 1430 (2003).
[23]C. Sauvan, G. Lecamp, P. Lalanne, and J. Hugonin, Opt. Express **13**, 245 (2005).
[24]P. B. Deotare, M. W. McCutcheon, I. W. Frank, M. Khan, and M. Loncar, Appl. Phys. Lett. **94**, 121106 (2009).
[25]K. Srinivasan, P. E. Barclay, M. Borselli, and O. Painter, Phys. Rev. B **70**, 081306(R) (2004).
[26]M. Notomi, A. Shinya, S. Mitsugu, E. Kuramochi, and H.-Y. Ryu, Opt. Express **12**, 1551 (2004).
[27]M. W. McCutcheon, G. W. Rieger, I. W. Cheung, J. F. Young, D. Dalacu, S. Frédérick, P. J. Poole, G. C. Aers, and R. L. Williams, Appl. Phys. Lett. **87**, 221110 (2005).
[28]C. P. Michael, M. Borselli, T. J. Johnson, C. Chrystal, and O. Painter, Opt. Express **15**, 4745 (2007).
[29]M. Galli, S. L. Portalupi, M. Belotti, L. C. Andreani L. OFaolain, and T. F. Krauss, Appl. Phys. Lett. **94**, 071101 (2009).
[30]S. M. Spillane, T. J. Kippenberg, O. J. Painter, and K. J. Vahala, Phys. Rev. Lett. **91**, 043902 (2003).
[31]P. E. Barclay, K. Srinivasan, and O. Painter, Opt. Express **13**, 801 (2005).
[32]F. Vollmer, D. Braun, A. Libchaber, M. Khoshsima, I. Teraoka, and S. Arnold, Appl. Phys. Lett. **80**, 4057 (2002).